16A.4 – OKLAHOMA TORNADOES OF 10 MAY 2010

Leslie R. Lemon[1,2] * , C.A. Van Den Broeke[1,2], C.D. Payne[1,2], P.T. Schlatter[2]

[1] *Cooperative Institute for Mesoscale Meteorological Studies (CIMMS), Norman, OK*

[2] *NOAA/NWS/Warning Decision Training Branch, Norman, OK*

1. Introduction

On 10 May 2010 an extremely dangerous combination of atmospheric ingredients developed over Kansas and Oklahoma producing approximately 65 tornadoes, along with many reports of very large hail and damaging straight-line winds. Many of the parent storms grew explosively and spawned these severe phenomena in very close proximity to a wealth of meteorological observing tools, especially weather radars. Included in these tools were three National Weather Service (NWS) S-band Weather Surveillance Radar - 1988 Doppler (WSR-88D) network radars (KTLX, KFDR, and KVNX), the Radar Operations Center's (ROC) WSR-88D test radar (KCRI), and the prototype dual-polarization WSR-88D, KOUN. Nearly collocated with KCRI and KOUN was an experimental phased array S-band radar. Additionally, the University of Oklahoma (OU) School of Meteorology (SOM) operated a C-band Enterprise dual-polarization radar (OU Prime) located very near to the National Weather Center (NWC) on the OU campus. A C-band Terminal Doppler Weather Radar (TDWR) was located approximately 25 km north of Norman. Finally, a network of four Collaborative Adaptive Sensing of the Atmosphere (CASA) X-band dual-polarization radars were located approximately 60 km to the southwest of Norman. Additionally, with the Norman NWS Weather Forecast Office (WFO) and the many other weather partners located in the NWC, there were many experienced and knowledgeable eyewitnesses to these storms.

We will only touch on some of the high points of storms on this day, focusing mainly on data from KVNX and KOUN. We will first begin with the observed tornadogenesis within the first Oklahoma supercell of the day in Oklahoma, the Wakita storm (A, Fig. 1). One of the most prominent features of the tornado was the "debris ball" or lofted debris associated with the tornado itself, but we will not confine our view to only one tornado associated debris ball but will consider the debris balls with several other storms. Where possible we will also consider the dual-polarization characteristics of the circulations and tornadoes. In addition to the debris ball with the tornadoes and tornado characteristics, we will also consider the relationship of the mesocyclones and tornadic vortices with the Z_{DR} columns and other dual-polarization variables, again where possible. While examining dual-polarization characteristics of some of these tornadoes we also discuss a "mysterious" area of echo in the wake of some tornado-bearing storms.

**Corresponding author address:* Les Lemon
120 David L. Boren Blvd Suite 2640
Norman, OK 73072
Email: les.lemon@noaa.gov

2. Overview

a. *Storm Environment*

A 500 mb westerly jet streak of 45 ms^{-1} moved out of the Texas panhandle into Oklahoma while a dryline at low-levels pushed eastward beneath the jet. Ahead of this dryline, near-surface winds were strong (~ 25 ms^{-1}) and backed with height while the low-level airmass was moist and steep mid-level lapse rates resulted in the airmass being very unstable with CAPE ranging from 3000 J/Kg to 4000 J/Kg. Deep layer wind shear (0-6 km AGL) was 30 to 40 ms^{-1} while the 0 to 1 km helicity increased from 250 Jkg^{-1} to 350 Jkg^{-1}.

The Storm Prediction Center (SPC) issued a high risk for severe thunderstorms, including strong, long-track tornadoes for central and eastern Oklahoman. By early afternoon a "particularly dangerous situation" tornado watch had been issued by the SPC covering all of central Oklahoma. These high-end NWS SPC products had been issued as a result of the potent synoptic and mesoscale conditions mentioned above.

b. *Storm Characteristics*

The first tornado-producing supercell storm of the day in Oklahoma began in the northwest part of the state in Roger Mills county about 1841 (all times UTC). The "Wakita" storm initially moved from 220° at 22.6 ms^{-1}. It then underwent a split and the southern, or right, member of the split became severe with a Weak Echo Region (WER) and a mid-level mesocyclone by about 1916. This supercell still displayed multicellular characteristics and its motion had turned to the right to 239° at 23.7 ms^{-1}. In fact, frequently storms that developed on this day were characterized by numerous cells developing preferentially on the right flank of the initially dominant storm. The result was numerous cell mergers, some beneficial and some detrimental, during the severe phase of each storms life.

While the Wakita storm moved northeast it was steadily approaching KVNX. This was the case with several storms and other radars in central Oklahoma on this day, i.e., developing or tornadic supercells passed very near or over radars. With decreasing range from the radar to a storm, more detail in its structure is able to be resolved due to decreasing beamwidth and therefore sample volume size. Moreover the radar horizon lowers with decreasing range to a storm allowing portions of the storm closest to the surface to be viewed as the storm approaches the radar. Finally, the minimum detectible signal is significantly lower very near the radar permitting the acquisition of information down to lower reflectivity despite somewhat higher spectrum widths. All these changes are generally beneficial to the meteorologist because an increasing number of radar gates sampled down to lower signal strength and nearer the surface translates into better storm structure resolution with all three moments of the radar.

As a storm approaches the radar it eventually moves into the cone of silence and less of the upper reaches of the storm are sampled by the radar. In other words, only progressively lower portions of the storm can be detected. In addition, as the storm moves very close to the radar each radial sample tends to distort and elongate features.

The Wakita storm began producing tornadoes virtually on top of the KVNX radar and moved northeast while other storms were rapidly developing in central Oklahoma. These storms quickly became supercellular and damaging. The NWS developed a map showing the tornadoes and identification scheme which we will follow here (Fig. 1).

3. Origins of the Wakita Storm "Debris Ball"

At 2025, as the southern edge of the Wakita storm passed 8.7 km to the northwest of the radar, the 19.5° antenna elevation angle showed a strongly convergent cyclonic shear zone (Fig. 2b) that was centered at 2800 m AGL and 7.9 km to the east-northeast of the radar. The mesocyclone velocity structure was nearly symmetric with a storm relative V structure of -24.7 ms^{-1} and +27.8 ms^{-1}.

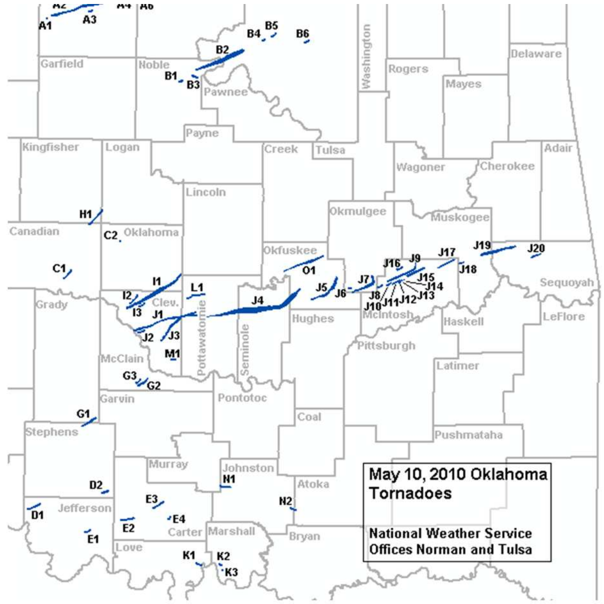

Figure 1: Tornado paths plotted using the alphabetical parent storm identifier and numbered in the order of tornado occurrence.

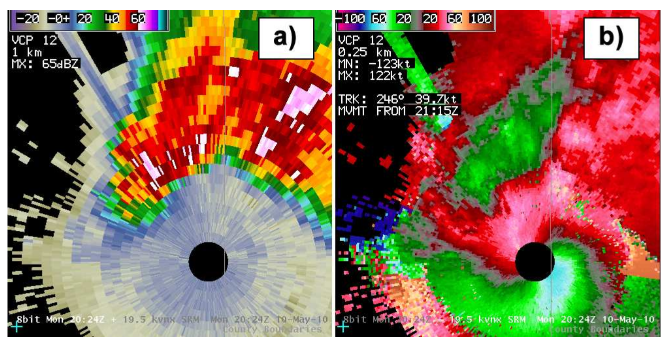

Figure 2: Image of reflectivity (Z: panel a) and storm-relative velocity (SRM: panel b) at 2025 UTC and 19.5 degrees elevation from the KVNX WSR-88D.

At 2029, the strong cyclonically sheared convergence zone continued was located at about 43 m AGL, 356° and at 5.5 km from the radar, mostly outside the precipitation region of the storm and in lower reflectivity (-1 to +25 dBZ). Ground-relative inflow (negative V, from the northeast) into this region and out of the storm precipitation cascade, was 15 ms^{-1} to 21 ms^{-1}. Southwest (+V) inflow into the cyclonic shear region from the Rear Flank Downdraft (RFD) was at about 7 ms^{-1} to 15 ms^{-1}. This shear zone may be a surface mesocyclone but it is too distorted and accompanied by high noise levels to be confidently identified as such.

However, by 2033 (Fig. 3a-b), a strongly convergent mesocyclone is present at 0.6° (~50 m AGL) with a total shear (ΔV) of 65 ms^{-1} (mean rotational V of 32 ms^{-1}). The

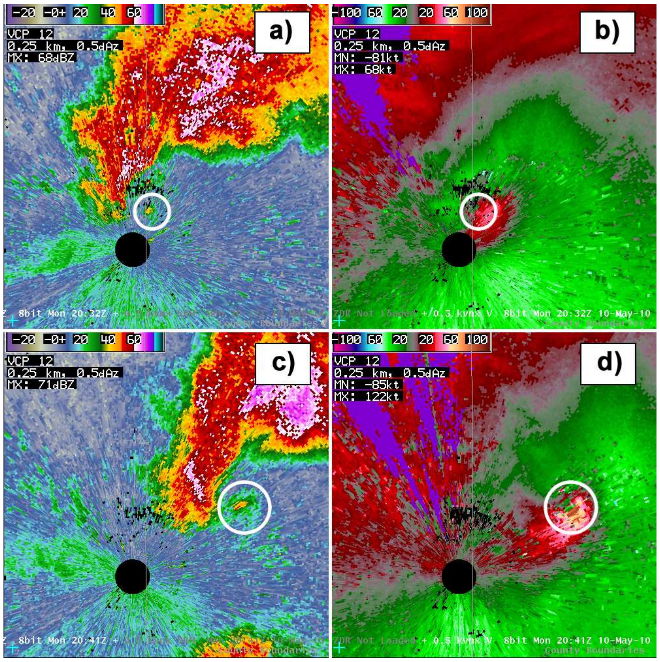

Figure 3: Time sequence of reflectivity (Z) and velocity (V) at 2033 and 2041 UTC. Panel (a) is Z at 2033 UTC, panel (b) is V at 2033 UTC, panel (c) is Z at 2041 UTC and (d) is V at 2041 UTC.

mesocyclone circulation is about 2.8 km across and is denoted by the white circle in Figure 3a-b. A possible TDS is centrally located in the shear region and is 1 km wide. In the literature (e.g. Kumjian and Ryzhkov (2008)) the TDS is composed of lofted debris by a tornadic circulation. This region of higher reflectivity (47 dBZ decreasing aloft) extends upward to over 500 m. However, the shear zone, or ΔV, across the possible TDS lacks the characteristic of a tornadic circulation even at 5 km from the radar. Moreover, the majority of the debris signature in low-levels is located in the region of the RFD and is associated with V values of +41 ms^{-1} to +44 ms^{-1} ground relative.

Thus, this region of enhanced reflectivity may be created by one or a combination of two causes. First, the enhanced reflectivity could be precipitation falling from aloft or it could be debris. It is unlikely that this is precipitation falling from aloft because reflectivity is highest in the lowest scan and decreases substantially and quickly aloft. Therefore, it would appear that the surface is the source of these echoes. Most of the echo is in the region of the RFD inflow "jet" (+31 ms^{-1} to +44 ms^{-1} ground relative) into the mesocyclone circulation so it appears the echo may actually be swept upward by the strong low-level winds of the RFD. This is further supported in the next volume scan where from the surface upward, a significant amount of the enhanced echo is again in the region of the maximum RFD velocity and not in the shear zone (not shown). However, the maximum reflectivity gates are in a high shear region near the center of the mesocyclone.

In the volume scans including and beyond 2041, this reflectivity core, is indeed centrally located in the high shear region of a tornadic-type signature (white circle, Fig. 3c-d). This is strong support for lofted debris by the tornadic vortex. However, this debris ball may have its origin within the RFD inflow "jet".

4. Mesocyclone Structure

Another important observation is the asymmetry of the mesocyclones for most of the storms on this day. This ground-relative asymmetry was driven by the dominance of the RFD flow over the inflow from the forward flank.

As an example, during the 2033 volume scan of the Wakita storm, the RFD flow was characterized by measured velocities of +41 ms^{-1} to +43.7 ms^{-1}, the flow from the Forward Flank Downdraft (FFD) and precipitation cascade was characterized by a V of -15 ms^{-1} to -23 ms^{-1}. During the 2041 volume scan the near surface (~160 meters) RFD winds had increased to +51.4 ms^{-1} to +65.8 ms^{-1} while flow from the FFD was still only -14 ms^{-1} to -24 ms^{-1}. As mentioned, this was not unique to the Wakita storm but was common with other mesocyclones and tornadoes on this day. The role of these strong RFD winds in producing damage at the surface was observed in at least two damage surveys.

Accounting for storm motion the circulations with this outbreak were far more symmetric in the storm relative reference frame. For example, in the 2041 volume scan and using the storm motion (typical for supercells on this day) of 251° and 41 ms^{-1}, peak storm relative velocity ranged from +45 ms^{-1} to – 44 ms^{-1}.

5. Tornadic Debris Signatures (TDS)

a. *Observation of a TDS*

The earliest inferred debris ball in the Wakita storm was developing by 2033 and extended vertically from the surface to about 570 m. The other possible debris areas in the RFD were confined to the lowest 200 to 300 m. This was similar to the 2037 volume scan except by that time the debris ball centered on the high-shear region had reached upward to over 2400 m. At that altitude the debris appears to merge with precipitation and cannot be discriminated from the same. However, that area is still centered on a high-shear signature with shear at that altitude being 76.7 ms^{-1} across a distance of about 1 km. Thus, it is still likely that some debris is mixed in with the precipitation.

Unambiguous identification of the debris ball can be solved, at least in part, with dual-polarization radar with the advent of the tornadic debris signature (TDS; Kumjian and Ryzhkov (2008)). In addition to high Z_H , low (or highly variable) Z_{DR} and ρ_{HV} usually less than 0.90 indicates that the echo is not meteorological, and if collocated with a velocity couplet, is indicative of debris lofted by a tornado. The addition of Z_{DR} and ρ_{HV} in the identification of tornadic debris is very helpful when precipitation begins mixing with the debris, as it does with KVNX. KVNX was not yet polarimetric for this case, so we used conventional judgment above as to the nature of the suspected echo. For other tornadoes located in central Oklahoma, however, we could use the KOUN radar located in Norman.

Figure 4 shows where there were four tornadoes sufficiently near the KOUN (and KTLX) radar. Note that with three of the tornadoes a TDS can be resolved in reflectivity alone, such that we are confident that these are damaging tornadoes. Note that there is further confirmation in the velocity data. However, there is one signature that we could not resolve in the reflectivity data, yet had a strong velocity signature. This is where dual-polarization data helped.

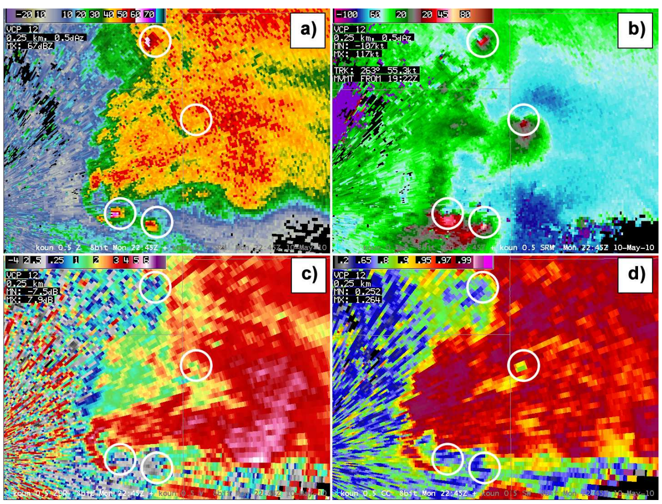

Figure 4: Image portraying the 4 tornadic debris signatures (TDS) occuring simultaneously. Panel (a) is reflectivity (Z), (b) is storm-relative velocity (SRM), (c) is differential reflectivity (Z_{DR}) and (d) correlation coefficient (ρ_{HV}).

When we turn our attention to the dual-polarization data, four TDSs can be resolved. It is especially clear from the ρ_{HV} values that are near or below 0.90, and as low as 0.65! When these ρ_{HV} values are correlated with sufficiently strong Z and with the velocity couplet, there is little doubt that we are observing a damaging tornado in progress.

Z_{DR} values are often low and negative in tornadic debris, but can be highly variable (as high as +2 dB). The variability of Z_{DR} is not surprising considering it is a function of type, amount, shape, and canting of the debris which itself varies as a function of the structures or vegetation struck and damaged by the tornado. For these reasons Z_{DR} values are primarily used as further supporting evidence of a TDS, once the low ρ_{HV} values in strong Z are identified.

There are two more concerns. One is that large hail can mimic the same characteristics as debris, especially if the Z_H values are high (e.g, 60 dBZ) and a velocity couplet is present. This is possible since the hook echo is often the location of large hail in addition to the tornado or damaging RFD winds. The second concern is three-body scatter spike (TBSS). Lemon (1998) indicated that the TBSS, when folded across the mesocyclone region can distort velocities. Similarly, three-body scattering can cause contamination of the dual-polarization variables down-radial of large hail. Thus, if the tornado is down-radial from a hail region, the three-body contamination can obscure the TDS in addition to the velocity signal. However, at this point it does appear that this problem will be rare.

b. *Vertical Extent of TDS*

We can also use the TDS to investigate the height of lofted debris within tornadic supercells. From observations following the tornadic storms of this day, banking checks and other documents were found over 100 km down stream/shear from their origin. It has been surmised that tornado debris is sometimes lofted to high altitude. With dual-polarization weather radar this can now be established (Fig. 5).

From the data accumulated here and especially from storm J (the "Norman" storm) we see good evidence that we have lofted debris and precipitation echo up to 9.4 km (31,000 feet) MSL (Table 1). We have continuity in the debris signature along with the vortex signature up to this height. Further, we have a tornado-associated "weak echo column" (like that identified by Lemon and Umscheid (2008) with the Greensburg, KS 2007 storm) collocated with the vortex and the debris signature. Thus, with the preponderance of the evidence pointing toward the presence of debris, we conclude that on this day and with storm J debris was lofted to at least 9.4 km MSL.

6. Vortices Aloft and Z_{DR} Columns

Storm I (the "Moore, OK" storm), prior to producing tornado I1 spawned a remarkable "chain" of both cyclonic and anticyclonic mesoscale vorticies in mid-levels along the storm rear quadrant (Fig. 6). At about 4600 m MSL we can arguably identify 4 mesoscale vortices along the rear echo flank of the Moore storm. These vortices are located along the rear edge of what is the BWER aloft and therefore associated with the primary and intense storm updraft. However, it is not apparent which, if any, of the vorticies will become dominant or possibly tornadic. With Z_{DR} though, something remarkable appears. Figure 7b-c indicates that only one of these circulations is directly associated with a Z_{DR} column

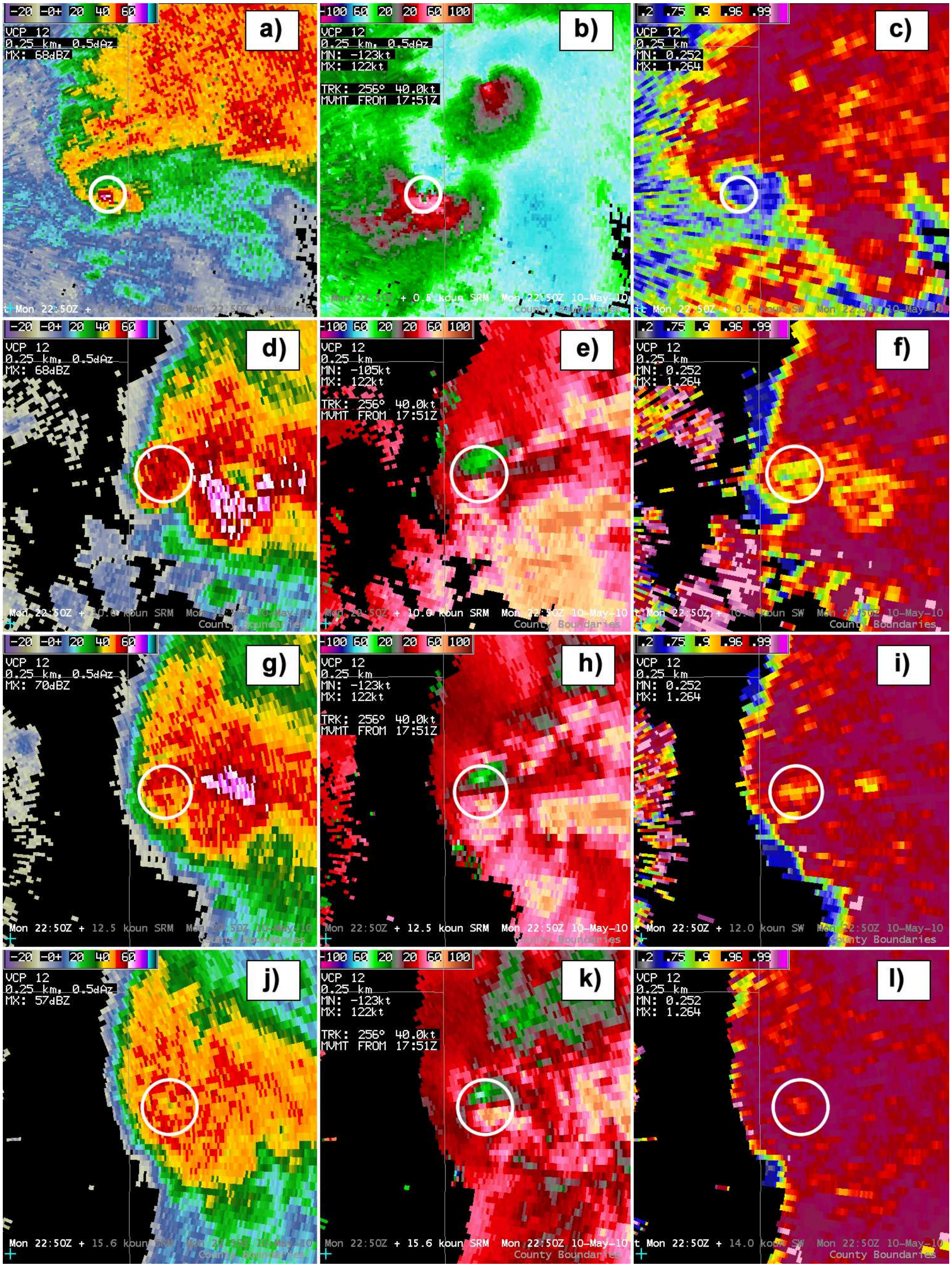

Figure 5: Shows the height extent of the TDS for the Norman storm (J1). The left-most images are reflectivity (Z). Middle set of images are storm-relative velocity (SRM) and the right-most images are ρ_{HV}. Panels (a-c) are for the elevation angle of 0.5 deg., (d-f) are for the elevation angle 10.0 deg., (g-i) are for the elevation angle of 12.5 deg., and panels (j-l) are for the elevation angle 15.6 deg.

Time (UTC)	Debris Signature?	Elevation (deg)	Height (km MSL)	Height (km AGL)
2229	N	—	—	—
2234	Y	12.5	2.66	2.32
2238	Y	15.6	4.99	4.65
2245	Y	12.5	6.90	6.57
2250	Y	15.5	9.57	9.23
2254	Y	1.3	1.22	0.88
2258	?	?	?	?
2303	Gone	—	—	—

Table 1: Evolution of the height of the highest discernable TDS in the dual-polarization data for the Norman tornado (J1).

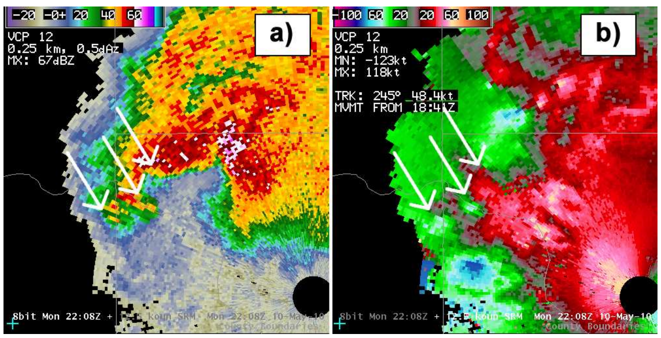

Figure 6: Image noting the multiple vortices (white arrows in panel b). A reflectivity image (panel a) is provided for reference.

(see Van Den Broeke et al. (2010)) and it is only that one circulation that goes on to be tornadic. It is worth noting, that a second vortex did appear along the southern side of the Z_{DR} column, but the vortex of interest was directly collocated with the Z_{DR} column.

The persistance of each of these vorticies would suggest that each is associated with vertical motion, whether updraft or downdraft. And the association of this circulation with the Z_{DR} column would suggest that it is associated with a significant updraft.

7. A “Mysterious” Echo

In Fig. 8b-d there is an ongoing tornado in progress (black arrow in figure). Note the area of rather strong echo to the rear of the tornado. This region is on the other side of the hook echo from the tornado and could be mistaken for rain or hail. The vertical extent of this echo is limited to 4.5 km in depth. Examining the dual-polarization variables (Fig. 8c-d), the ρ_{HV} values are well below 0.90 and the Z_{DR} is near 0 dB. Therefore, this echo has the unmistakable character of non-precipitation echo. What is the origin of this echo?

Debris in the wake of tornadoes have been observed in these same locations in previous studies (Magsig and Snow

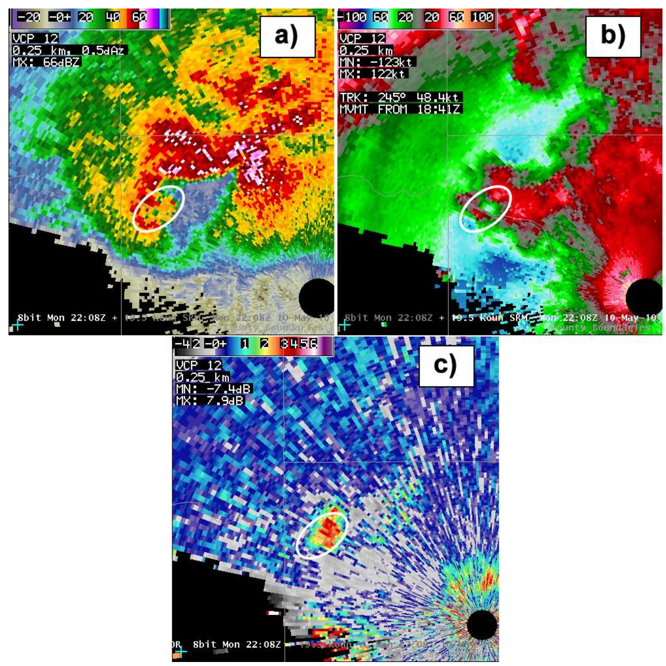

Figure 7: Image depicting the only velocity couplet in the string of couplets to be associated directly with a Z_{DR} column. Panel (a) is reflectivity (Z), panel (b) is storm relative velocity (SRM) and panel (c) is differential reflectivity (Z_{DR}).

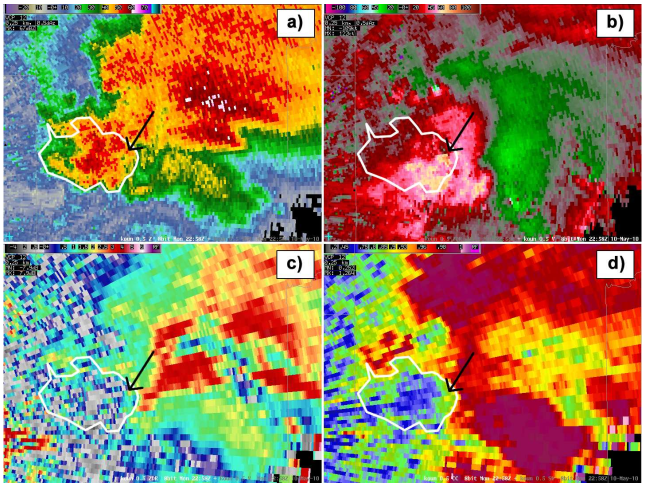

Figure 8: Depiction of the "mystery" echo. Reflectivity (Z) is in the top left panel, differential reflectivity (Z_{DR}) is in the lower left panel, velocity (V) is in the upper right panel and correlation coefficient (ρ_{HV}) is in the lower right panel.

(1998)). Storm-relative velocities in this region are divided between flow away from the storm on the north side to light flow toward the storm on the south side (not shown). One of the authors observed leaves lofted in the RFD after the passage of the tornado in Norman very early in the tornado life cycle. Leaves were also observed falling out in the wake of a later tornado near Seminole, OK (personal communication – Robin Tanamachi). There are not any available observations of the echo during this volume scan, however, so it is not clear what the scatterers are. At this time, the echo remains mysterious.

8. Summary

This brief observational examination presents several situations where dual-polarization variables contributed significantly to our analysis. Additionally, there were some radar observations that were presented that are not fully understood at this time. However, every remote sensing device has a long learning curve and dual-polarization weather radar is no exception. Overall, this does suggest that as our atmospheric sampling increases we are again opening a new "window" on the atmosphere.

9. Acknowledgments

The authors would like to thank the Warning Decision Training Branch (WDTB) for providing resources to conduct this research. Also, this extended abstract was prepared by Les Lemon, Clark Payne and Cynthia Van Den Broeke with funding provided by NOAA/Office of Oceanic and Atmospheric Research under NOAA-University of Oklahoma Cooperative Agreement #NA17RJ1227, U.S. Department of Commerce. The statements, findings, conclusions, and recommendations are those of the author(s) and do not necessarily reflect the views of NOAA or the U.S. Department of Commerce.

References

Kumjian, M. R. and A. V. Ryzhkov, 2008: Polarimetric signatures in supercell thunderstorms. *J. Appl. Meteor. Climatol.*, **47**, 1940–1961.

Lemon, L. R., 1998: The radar "three-body scatter spike": An operational large-hail signature. *Wea. Forecasting*, **13**, 327–340.

Lemon, L. R. and M. Umscheid, 2008: The Greensburg, KS tornadic storm: A storm of extremes. *Extended Abstracts, 24th Conf. on Severe Local Storms*, Savannah, GA, Amer. Meteor. Soc., 1–19.

Magsig, M. A. and J. T. Snow, 1998: Long-distance debris transport by tornadic thunderstorm Part I: The 7 May 1995 supercell thunderstorm. *Mon. Wea. Rev.*, **126**, 1430–1449.

Van Den Broeke, C. A., C. D. Payne, L. R. Lemon, and P. T. Schlatter, 2010: Zdr column characteristics and trends during the 10 May 2010 severe weather outbreak. *Extended Abstracts, 25th Conf. on Severe Local Storms*, Denver, CO, Amer. Meteor. Soc., 1–4.